The American Journal of Pathology, Vol. 182, No. 4, April 2013

The American Journal of
PATHOLOGY
ajp.amjpathol.org

IMMUNOPATHOLOGY AND INFECTIOUS DISEASES

CD44 Deficiency Contributes to Enhanced Experimental Autoimmune Encephalomyelitis

A Role in Immune Cells and Vascular Cells of the Blood–Brain Barrier

Kelly M. Flynn,*† Michael Michaud,* and Joseph A. Madri*

From the Departments of Pathology and Cell Biology,† Yale University School of Medicine, New Haven, Connecticut*

Accepted for publication January 3, 2013.

Address correspondence to Joseph A. Madri, Ph.D., M.D., Department of Pathology, Yale University School of Medicine, 310 Cedar St., P.O. Box 208023, New Haven, CT 06520-8023. E-mail: joseph.madri@yale.edu.

Adhesion molecule CD44 is expressed by multiple cell types and is implicated in various cellular and immunological processes. In this study, we examined the effect of global CD44 deficiency on myelin oligodendrocyte glycoprotein peptide (MOG)-induced experimental autoimmune encephalomyelitis (EAE), a murine model of multiple sclerosis. Compared to C57BL/6 wild-type mice, CD44-deficient mice presented with greater disease severity, increased immune cell numbers in the central nervous system, and increased anti-MOG antibody and proinflammatory cytokine production, especially those associated with T helper 17 (Th17) cells. Further, decreased numbers of peripheral $CD4^+CD25^+FoxP3^+$ regulatory T cells (Tregs) were observed in CD44-knockout mice throughout the disease course. CD44-knockout CD4 T cells exhibited reduced transforming growth factor-β receptor type I (TGF-β RI) expression that did not impart a defect in Treg polarization *in vitro*, but did correlate with enhanced Th17 polarization *in vitro*. Further, EAE in bone marrow–chimeric animals suggested CD44 expression on both circulating and noncirculating cells limited disease severity. Endothelial expression of CD44 limited T-cell adhesion to and transmigration through murine endothelial monolayers *in vitro*. Importantly, we also identified increased permeability of the blood–brain barrier *in vivo* in CD44-deficient mice before and following immunization. These data suggest that CD44 has multiple protective roles in EAE, with effects on cytokine production, T-cell differentiation, T-cell–endothelial cell interactions, and blood–brain barrier integrity. *(Am J Pathol 2013, 182: 1322–1336; http://dx.doi.org/10.1016/j.ajpath.2013.01.003)*

Multiple sclerosis (MS) is an autoimmune, demyelinating disease resulting from chronic inflammation in the central nervous system (CNS). Experimental autoimmune encephalomyelitis (EAE), the primary and long-used animal model of MS, produces immune processes relevant to the human disease.[1] The progression and pathogenesis of EAE is complex and depends on multiple cell types and processes.[2–4]

T helper 17 (Th17) cells and their distinctive cytokine, IL-17, play pivotal roles in EAE/MS pathogenesis.[5–7] Th17 cells, members of a CD4 T-cell effector subset, are generated from naive CD4 T-cell precursors in response to cytokines TGF-β and IL-6, whereas IL-23 expands this population and increases pathogenicity.[8,9] In EAE, Th17 cells first infiltrate and initiate recruitment to the CNS,[5,6] and Th17-produced IL-17 induces neuronal death[6] and increases permeability of the blood–brain barrier (BBB), allowing continued influx of immune cells by disrupting endothelial cell (EC) junctions.[6,10]

Regulatory T cells (Tregs), the primary suppressors of the immune system, play a pivotal role in EAE that is opposite to Th17 cells. Treg depletion exacerbates disease symptoms, whereas supplementation with additional Tregs ameliorates

Supported in part by US Public Health Service grants R37-HL28373, RO1-HL51018, and a Reed Foundation grant (J.A.M.) and by NIH grants T32 GM007223 and T32 DK07556 (K.M.F.).

http://dx.doi.org/10.1016/j.ajpath.2013.01.003

the disease.[11,12] Identified by the expression pattern $CD4^+CD25^+FoxP3^+$, Tregs are generally divided into two principal subsets: naturally occurring Tregs, which arise in the thymus during development, and induced Tregs (iTregs), which can be generated in the periphery from naive CD4 T cells in response to TGF-β.[13,14]

Vascular EC also contribute to the complex pathogenesis of EAE. EC regulate leukocyte adhesion and extravasation, maintain vascular integrity, and limit injury and immune-mediated vascular permeability. The CNS vasculature, the primary constituent of the BBB, is especially unique and plays a critical role in protecting the CNS microenvironment. In MS/EAE, there is a characteristic breakdown of the BBB followed by accumulation of inflammatory infiltrates.[15,16]

CD44, a ubiquitously expressed type I transmembrane glycoprotein, has been implicated in a wide variety of cellular processes within and outside of the immune system.[17,18]Alternative splicing and multiple posttranslational modifications generate various structural and functional versions of CD44 and are thought to be responsible for its large range of diverse and sometimes seemingly contradictory cellular functions.

Although CD44 has been studied in several immunological contexts as a positive or negative regulator of inflammation, the many results are confounded by use of different mouse strains, inflammatory models, and experimental approaches. CD44 has been implicated as a proinflammatory molecule in several studies that identified an anti-inflammatory effect of a CD44 monoclonal antibody in multiple immune-mediated processes and diseases such as lymphocyte extravasation,[19]collagen- or proteoglycan-induced arthritis, respectively,[20,21] type 1 diabetes,[22] asthma,[23] and EAE.[24] However, most studies in CD44-knockout (KO) mice suggest an anti-inflammatory role for this molecule in various immunological processes instead. CD44-KO mice experience enhanced inflammation in several models of pulmonary inflammation that suggest various roles of CD44 in immune cell clearance, TGF-β signaling, and repression of Toll-like receptor (TLR) signaling and inflammatory gene expression.[25–28] Further, CD44-KO mice show increased septic responses to lipopolysaccharide[29] and enhanced inflammatory responses following myocardial infarction[30] or hepatic injury.[31] CD44 deficiency also led to increased collagen-induced arthritis severity with up-regulation of inflammatory genes in arthritic CD44-KO T cells.[32] Clearly, antibody-mediated interference can have very different effects than genetic disruption of CD44. Hutas et al[33] in 2008 reported disparate effects of CD44 monoclonal antibody treatment versus CD44 deficiency on leukocyte recruitment during proteoglycan-induced arthritis.

Despite antibody-mediated interference studies, the role of CD44 in EAE/MS remains poorly understood. In active MS lesions, there is an increase in CD44 expression and accumulation of hyaluronan (HA), a major CD44 ligand.[34,35] Previously, CD44 was shown to facilitate uptake of HA,[36] promoting resolution of tissue-injury signals and inflammation.[25,37] By contrast, a conditional mouse model of oligodendrocyte-specific overexpression of CD44 found a correlation between CD44 expression and enhanced HA accumulation, prevention of oligodendrocyte differentiation, and subsequent inflammation-independent demyelination.[35]

Until recently, EAE had not been examined in CD44-KO mice. This report demonstrates that CD44-KO mice present with increased EAE disease severity. This was associated with loss of CD44 on circulating immune cells, and also on noncirculating cells, specifically vascular EC of the BBB. We illustrate a more proinflammatory T-cell profile in CD44-KO mice with a reduction in Treg numbers throughout the disease that is accompanied by increased permeability of the BBB. Further, we illustrate a previously unidentified role for CD44 in the baseline integrity of the BBB, which has far-reaching implications beyond MS/EAE.

Materials and Methods

Mice and Reagents

C57BL/6 wild-type (WT) and CD44-KO mice (B6.129 (Cg)-*Cd44*^{tm1Hbg}/J) (The Jackson Laboratory, Bar Harbor, ME) were housed in the animal facilities at Yale University School of Medicine according to Yale University and NIH guidelines. All mice were used between 8 and 10 weeks of age. Murine MOG_{35-55} peptide was synthesized by the W.M. Keck Biotechnology Resource Laboratory at Yale University (New Haven, CT). Alexafluor-conjugated secondary antibodies were purchased from Invitrogen (Carlsbad, CA) and horseradish peroxidase—conjugated secondary antibodies from Santa Cruz Biotechnology (Santa Cruz, CA). Fluorescent-conjugated primary antibodies anti-CD4, anti-CD25, anti-CD45, anti-FoxP3, and anti—IL-17 were purchased from BD Bioscience (San Jose, CA). Anti-TGFβRI was purchased from Santa Cruz Biotechnology. Anti-CD31 was generated in house previously.[38]

EAE Induction

Unless otherwise stated, mice received 300 μg of rodent MOG_{35-55} peptide emulsified in complete Freund's adjuvant containing heat-killed *Mycobacterium butyricum* (Difco, Detroit, MI) via s.c. flank injection on days 0 and 7; on days 0 and 2, mice received 500 ng of pertussis toxin (List Biological Laboratories, Campbell, CA) via i.p. injection. The mice were monitored daily and graded for clinical symptoms of EAE on the following basis: 0, no disease; 1, flaccid tail; 2, hind-limb weakness/unsteady gait; 3, hind-limb paralysis; 4, hind- and fore-limb weakness/paralysis; 5, moribund. Disease index was calculated by [(sum of the mean daily clinical scores)/(day of disease onset)] × 100.

Histopathology and Immunofluorescence

Mice were deeply anesthetized and perfused intracardially with cold PBS followed by room temperature formalin

(paraffin sections) or cold 4% paraformaldehyde in PBS (frozen sections). Brains and spinal cords were removed and fixed in formalin or 4% paraformaldehyde. Paraffin-embedded tissues were processed, sectioned, and stained with H&E by the Research Histology Laboratory at Yale. For immunofluorescent staining, tissues were embedded in optimal cutting temperature compound and cut into 6-μm thin sections for CD45 staining or 40-μm-thick sections for IgG/CD31. Before staining, sections were washed with PBS and blocked for 1 hour at room temperature with 1% bovine serum albumin, 3% normal goat serum, and 0.3% Triton X-100 in PBS. Thin sections were incubated with rat anti-CD45 (BD Bioscience) for 2 hours at room temperature, followed by goat anti-rat IgG conjugated to alexafluor-594. Thick floating sections were incubated with goat anti-mouse IgG conjugated to alexafluor-594 and rabbit anti-CD31 for 48 hours at 4°C followed by goat anti-rabbit IgG conjugated to alexafluor-488.

Antibody Enzyme-Linked Immunosorbent Assay

For serum collected from WT and CD44-KO mice during EAE, 96-well plates were coated with 10 μg/mL MOG_{35-55} peptide in PBS overnight at 4°C. Serum was collected, diluted 1:1000 in PBS containing 1% bovine serum albumin, and incubated on MOG-coated plates for 2 hours at room temperature, followed by anti-mouse IgG conjugated to horseradish peroxidase secondary antibodies. Signal was visualized with tetramethylbenzidine substrate and detected on a Wallac multiplate reader (PerkinElmer Life Sciences, Shelton, CT) at 450 nm.

Isolation of CNS Mononuclear Cells

To isolate mononuclear cells from the inflamed CNS, mice were deeply anesthetized and perfused intracardially with cold RPMI. CNS tissue was removed, homogenized, incubated with 1 mg/mL collagenase at 37°C for 30 minutes, and then centrifuged over a discontinuous Percoll gradient by resuspending the resulting pellet in 3 mL of 100% Percoll, then layering the suspension with 2 mL of 80% Percoll, 3 mL of 40% Percoll, and 2 mL of 30% Percoll. Percoll (100%) was made by adding 9 mL of Percoll and 1 mL of 10× PBS. All other dilutions were made from 100% Percoll and 1× PBS. Isolated cells were counted and immediately used for RNA extraction and cDNA preparation. CNS tissue from six mice was pooled for each sample.

Microglial cells from individual bone marrow (BM)-chimeric mice were isolated as previously described.[39]

RNA Extraction, cDNA Preparation, and Real-Time PCR

RNA was extracted from cells using an RNeasy Protect Mini Kit (Qiagen, Valencia, CA) and cDNA generated from 750 ng of RNA using an iScript cDNA Synthesis Kit (Bio-Rad, Hercules, CA) as per the manufacturer's instructions. Real-time PCR was performed using SYBR Green Supermix (Bio-Rad) and 1 μL of cDNA per sample (each sample was run in triplicate). Ct values were normalized against β-actin, and data were analyzed using the ΔΔCt method. Validated primers were ordered from Real Time Primers (Elkins Park, PA) with the exception of the IL-17A and TGFβRI primers, which were synthesized by Integrated DNA Technologies (Coralville, IA). Primer sequences are as follows: IL-17A (forward) 5′-ACCTCAACCGTTCCACGTCA-3′, (reverse) 5′-CAGGGTCTTCATTGCGGTG-3′; TGFβRI (forward), 5′-CATTCACCACCGTGTGCCAAATGA-3′, (reverse) 5′-ACCTGATCCAGACCCTGATGTTGT 3′.

T-Cell Restimulation and Cytokine Measurement

Splenocytes were isolated and cultured in RPMI supplemented with 10% fetal bovine serum. Splenocytes (3.5×10^6) were cultured in 24-well plates with 50 μg/mL MOG_{35-55}, and the supernatant was collected after 72 hours. Cytokine enzyme-linked immunosorbent assays (ELISAs) (eBioscience, San Diego, CA) were performed as per the manufacturer's instructions. Each sample was completed in triplicate.

Flow Cytometry

Splenocytes or lymph node cells from naïve or immunized animals were prepared for fluorescence-activated cell sorting (FACS) as previously described.[40] For Tregs, fixation and FoxP3 staining using a FoxP3 Staining Kit (eBioscience) was performed as per the manufacturer's instructions, using CD4 and CD25 fluorescently conjugated antibodies. For intracellular IL-17 detection, cells were cultured for 5 hours with 50 ng/mL phorbol myristate acetate, 500 ng/mL ionomycin (Sigma-Aldrich, St. Louis, MO), and GolgiStop Protein Transport Inhibitor (BD Bioscience). The cells were first stained for surface markers, followed by fixation, permeabilization, and staining with fluorescently conjugated anti−IL-17 using a Cytofix/Cytoperm Fixation/Permeabilization Solution Kit (BD Bioscience). Flow cytometric analysis was performed using a FACSCalibur or LSR II flow cytometer and FlowJo software (all from BD Bioscience).

Cell Lysate Preparation and Western Blot Analysis

Splenic and T-cell lysates were prepared and subjected to Western blot analysis as described previously.[40]

CD4 T-Cell *in Vitro* Polarization

Naive CD4 T cells were isolated from total splenocytes using an EasySep Mouse $CD4^+$ T Cell Enrichment Kit (Stemcell Technologies, Vancouver, BC, Canada) as recommended by the manufacturer. CD4 T cells (0.75×10^6) were stimulated with plate-bound anti-CD3 and soluble anti-CD28 (BD Bioscience) at 1 μg/mL each. For Treg differentiation, cells were treated with 20 ng/mL IL-2 (R&D

Systems, Minneapolis, MN) and 2 to 10 ng/mL TGF-β (PeproTech, Rocky Hill, NJ). For Th17 differentiation, cells were treated with 20 ng/mL IL-6 (eBioscience), 20 ng/mL IL-23 (eBioscience), 5 ng/mL TGF-β, 10 μg/mL anti−IL-4 (eBioscience), and 10 μg/mL anti−interferon (IFN)-γ (eBioscience) with or without 50 μg/mL low molecular weight (LMW) or 50 μg/mL high molecular weight (HMW) HA (Sigma-Aldrich). After 96 hours, cells were prepared for FACS analysis as described above.

Generation of BM Chimeras

Hematopoietic precursor transplantation was performed as described previously.[41] Briefly, recipient mice were irradiated twice with 5 Gy (500 rads) separated by 2 hours, using a ^{137}Cs irradiator. Six hours after the second irradiation, recipient mice received 12×10^6 donor marrow cells retro-orbitally. After 6 weeks, cells were harvested from chimeric animals as described or EAE was induced.

Murine BrEC Isolation and Culture

Cerebral capillary EC were isolated from brain microvessels of 4- to 10-day-old WT and CD44-KO mice, and immortalized as described previously.[41] Murine brain EC (BrEC) were cultured on 1.5% gelatin−coated plates in Dulbecco's modified Eagle's medium containing 10% fetal bovine serum, 2 mmol/L L-glutamine, 0.1 mmol/L nonessential amino acids, 1 mmol/L sodium pyruvate, 10 mmol/L HEPES, 10^{-5} mol/L β-mercaptoethanol, 100 U/mL penicillin, and 100 μg/mL streptomycin in 8% CO_2 at 37°C. Cells were used between passages 10 and 15.

Adhesion and Transendothelial Migration Assay

T-cell adhesion to EC was examined as previously described.[40] Twenty-four hours before lymphocyte addition, the BrEC medium was changed to 1% fetal bovine serum in Dulbecco's modified Eagle's medium with or without 10 ng/mL murine TNFα (PeproTech). Unstimulated or anti-CD3/anti-CD28−activated T cells (1×10^6) were added to the BrEC monolayers in serum-free Dulbecco's modified Eagle's medium and incubated at 37°C for 5 hours. For hyaluronidase treatment, BrEC were incubated with 0.5 U/mL hyaluronidase (from *Streptomyces hyalurolyticus*; Sigma-Aldrich) in serum-free medium for 1 hour at 37°C before addition of T cells.

T-cell transendothelial migration was performed as previously described using a Transwell system (BD Bioscience).[40] Anti-CD3/anti-CD28−activated T cells (1.6×10^6) were added to the upper well containing a confluent BrEC monolayer in serum-free Dulbecco's modified Eagle's medium. T cells that migrated through the BrEC monolayer and underlying extracellular matrix were collected from the lower chambers at 4, 20, and 40 hours and counted.

In Vivo Evans Blue Permeability Assay

In vivo permeability was measured by 4 μL/g bodyweight retro-orbital injection of sterile 0.5% Evans Blue dye w/v in PBS as described previously.[41] One hour following the injection of dye, mice were anesthetized, perfused intracardially with cold PBS, and brains were removed. Dye was extracted from minced brain tissue by incubating the tissue in 5 μL/mg tissue formamide at room temperature for 72 hours. The optical density at 650 nm ($OD_{650\ nm}$) value was measured for each sample, and a permeability index was calculated by dividing the $OD_{650\ nm}$ value for each sample by the average $OD_{650\ nm}$ value of tissue from three mice that had not received dye. Skin vessel permeability was determined similarly.

Statistical Analysis

Differences between data sets were analyzed using *P* values determined using a two-tailed Student's *t*-test. Error bars represent SEM.

Results

Deletion of CD44 Results in Increased EAE Disease Severity and Inflammation

To examine the effect of CD44 deficiency during MOG-induced EAE, C57BL/6 WT and CD44-KO mice were immunized with MOG_{35-55} peptide, and several disease processes were characterized. First, the mice were monitored daily for clinical symptoms of EAE. The WT and CD44-KO animals displayed a similar onset and progression of the disease, with first clinical symptoms appearing around day 11 and peaking around day 18. However, the CD44-KO mice exhibited significantly increased disease severity as evidenced by clinical disease scores, disease index, and mortality (Figure 1, A−C, and Table 1). A recent study suggested diminished EAE severity in CD44-KO mice.[42] To confirm our findings and identify reasons for this discrepancy, we used several additional EAE immunization protocols, including the identical protocol of that study, as well as using a distinct and independently derived strain of CD44-KO mice.[25,27] Under each circumstance, we found increased EAE disease severity in the CD44-KO strain compared to WT counterparts (Supplemental Figure S1 and Supplemental Table S1).

To evaluate quantities of immune cell within the CNS parenchyma, brain and spinal cord tissue was isolated from WT and CD44-KO animals near the peak of disease. Immunofluorescent analysis revealed significantly increased numbers of immune cells ($CD45^+$) in the spinal cords of the CD44-KO animals compared to WT that was further corroborated using H&E staining (Figure 1D). Compared to WT, there were also greater numbers of CD4 T cells found in the spinal cords of CD44-KO by immunofluorescence (Figure 1E). On average, 1.20×10^6 mononuclear cells

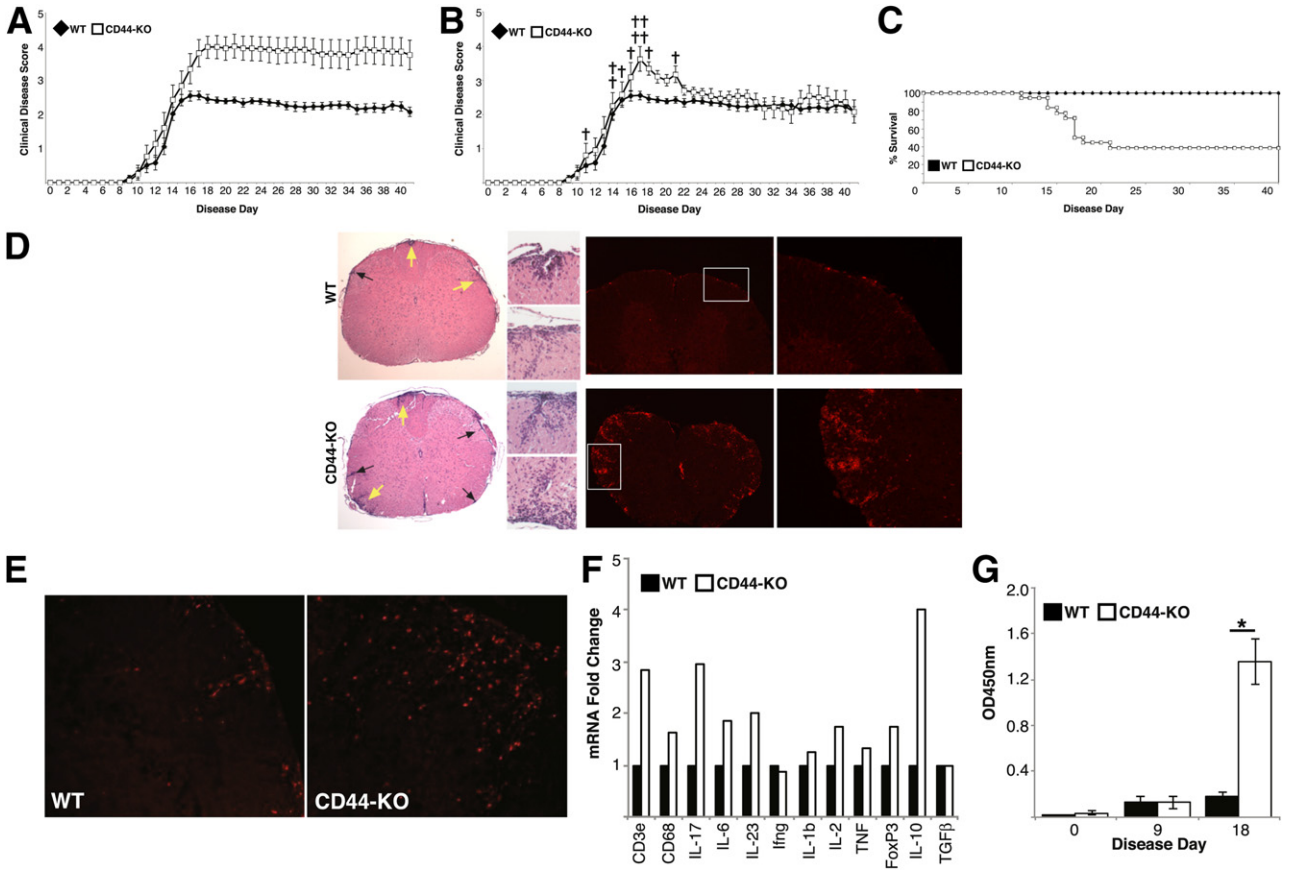

Figure 1 CD44-KO mice suffer from increased EAE disease severity and show enhanced disease characteristics. **A:** Average clinical disease scores of WT and CD44-KO mice following induction of EAE, where mortality scores are included in average score from time of death throughout the study. Data represent two independent experiments with combined $n = 21$ for WT, $n = 18$ for CD44-KO. Data are expressed as means ± SEM. **B:** Clinical disease curve, where mortality scores are included in average score only on day of death and excluded from subsequent days. †CD44-KO death. **C:** Kaplan-Meier survival curve. **D:** Representative H&E stain (**left panels**) and CD45 immunofluorescence (**right panels**) of WT (**top row**) and CD44-KO (**bottom row**) lumbar spinal cord, ×4 magnification, at day 20 ($n = 3$ for each). **Arrows** indicate inflammatory infiltrates; Regions indicated by **yellow arrows** and **insets** are shown at higher magnification (×20). **E:** Representative CD4 immunofluorescence of WT and CD44-KO lumbar spinal cord at day 20 ($n = 3$ for each). **F:** Real-time PCR analysis of mononuclear cell RNA isolated from inflamed CNS (day 20) for immune cell markers and cytokines. Six spinal cords were pooled for each strain sample, and samples were run in triplicate. Data are presented as ΔΔCt fold change. **G:** Measurement of relative levels of anti-MOG antibody by ELISA. Data are presented as means ± SEM with $n = 4$ per group. $^*P = 0.001$.

were isolated from the inflamed WT CNS, whereas 1.84×10^6 were isolated from the CD44-KO. Quantitative real-time PCR analysis of RNA isolated from these cells showed greater quantities of lymphoid and activated microglial/macrophage cells (CD3e, CD68) and cytokine mRNAs (Figure 1F).

Finally, serum collected from WT and CD44-KO mice was assessed for relative levels of total anti-MOG IgG at day 0 (pre-immune, naïve), day 9, and day 18. No significant differences were observed between the WT and KO IgG production in the naïve or early disease state. However, by day 18, the CD44-KO mice had significantly more serum anti-MOG IgG than the WT mice (Figure 1G).

CD44-KO Mice Have Increased Proinflammatory T-Cell Profiles during EAE

CD4 T cells are critical initiators and mediators of EAE. We examined the characteristics of the T cells in the periphery to identify potential causes of the increased inflammation in

Table 1 EAE Clinical Disease Characteristics

Mouse strain	Average day disease onset	Average maximum disease score	Sum daily average disease score	Disease index (40 day)	Percent mortality
WT	12.6	2.80*	67.11	494.47**	0
CD44-KO	12.7	4.18*	109.42	798.32**	61

EAE disease measurements from WT and CD44-KO mice. Disease index, a measure of when and how sick the animals become, is calculated by (sum of the mean daily disease score/mean day onset) × 100.

$^*P = 0.0003$, $^{**}P < 0.0001$.

the CD44-KO CNS. In the naïve state, the T-cell populations (Figure 2A), as well as their MOG-specific cytokine production (data not shown), were comparable between the two strains.

When we examined splenic cytokine production in response to MOG stimulation at several times during the course of the disease (days 9, 15, 18, and 28), we found significantly increased production of Th17-associated cytokines, strongly suggesting a greater number of Th17 cells, in the CD44-KO throughout the duration of the disease (Figure 2B). Further, a trend toward increased proinflammatory cytokine IFN-γ was also observed.

We postulated that the increased proinflammatory milieu observed in the CD44-KO could be the result of impaired immune suppression owing to decreased numbers or function of Tregs. Importantly, the CD44-KO mice had significantly lower numbers of splenic Tregs throughout the disease (Figure 2C).

CD44-KO CD4 T Cells Express Lower Levels of TGFβRI and Exhibit Altered CD4 T-Cell Polarization *in Vitro*

The paucity of splenic Tregs in CD44-KO mice during EAE, despite similar numbers before disease induction (Figure 2, A and C), suggested a potential defect in iTreg differentiation. We postulated that this paucity could be due to defective TGF-β signaling and/or increased Th17 populations. Because no differences were noted in TGF-β cytokine levels (Figure 2B), we examined surface protein expression of the three TGF-β receptors (TGFβR) on WT and CD44-KO splenocytes. No appreciable difference was observed in TGFβRII or TGFβRIII expression (data not shown). However, the CD44-KO splenocytes showed significantly lower expression of TGFβRI, both at the cell surface as detected by FACS (Figure 3A) and in whole-cell lysates as detected by Western blot (Figure 3B). The decreased expression was specific to CD4 T cells, as no significant differences were seen when comparing CD4 T-cell–depleted samples (Figure 3B). Further, despite difference in TGFβRI protein expression, there was no alteration in mRNA level (Figure 3C).

Lower expression of TGFβRI could alter TGF-β signaling, leading to aberrant Treg polarization and loss of iTregs *in vivo*. However, because TGF-β signaling is also required for the differentiation of Th17 cells, it is possible that CD44-KO cells have abnormal polarization to this effector subtype as well, which could also prevent appropriate Treg differentiation. To test these theories, we isolated naïve CD4 T cells and subjected them to Treg or Th17 polarizing conditions *in vitro*. WT and CD44-KO CD4 T cells showed similar TGF-β dose-dependent increases in Treg differentiation. However, the CD44-KO cells showed a significantly enhanced polarization to the Th17 phenotype compared to WT (Figure 4). Small amounts of Treg differentiation occurred under Th17 polarizing conditions in both WT and CD44-KO samples, but no significant differences were observed in this population (data not shown). Under Treg-polarizing conditions, there was no induction of Th17 cells in WT CD4 T cells, though a slight increase was observed in the Th17 population in the CD44-KO CD4 T cells.

To determine whether addition of CD44 ligand altered the development of Th17 cells, we examined Th17 polarization

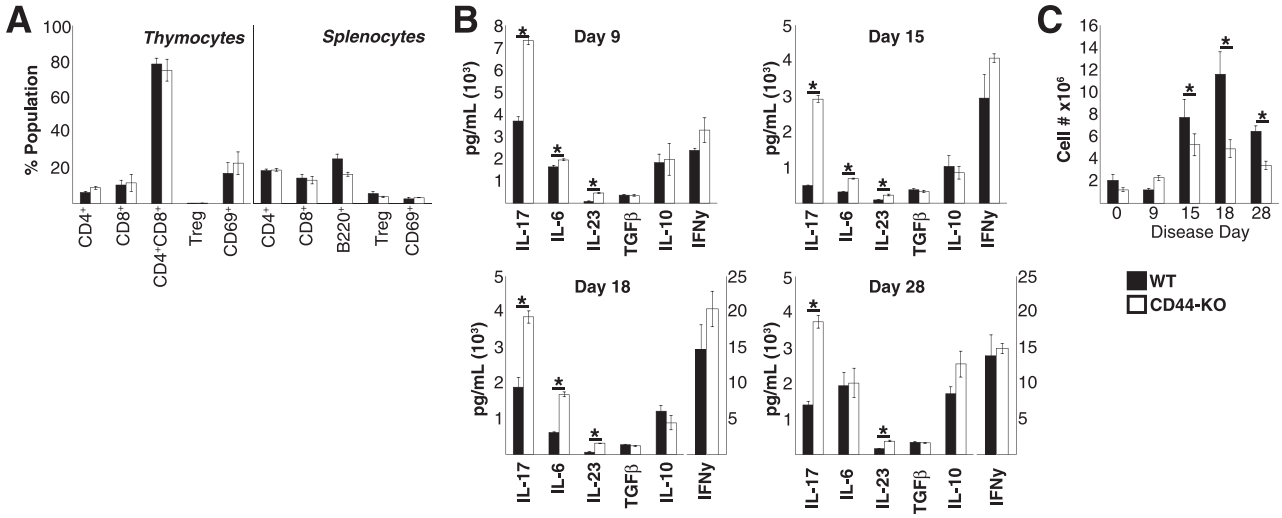

Figure 2 CD44-KO mice produce greater amounts of proinflammatory cytokines, especially those associated with Th17 cells, and lower number of Tregs than WT mice during EAE. **A**: WT and CD44-KO mice contain similar numbers of thymocytes and splenocytes, with similar cell-type distribution in the naïve state by FACS. Tregs are identified as $CD4^+CD25^+FoxP3^+$ cells. $CD4^+CD69^+$ cells are gated on CD4. Data are representative of two independent experiments with a total $n = 6$ per strain and are expressed means ± SEM. **B**: Splenocytes isolated from immunized animals at indicated day were stimulated with MOG_{35-55} peptide, and Ag induction of cytokines was measured via ELISA. Splenocytes were isolated independently from six animals per strain at indicated time points, and each supernatant was run in triplicate. Data are expressed as means ± SEM. IFN-γ levels on days 18 and 28 are on a distinct scale in pg/mL. **C**: Quantitative FACS analysis of splenic $CD4^+CD25^+FoxP3^+$ regulatory T cells during EAE. For each day, splenocytes were isolated from six animals per strain. Data are expressed as means ± SEM. $^*P < 0.01$, $^{**}P < 0.005$, and $^{***}P < 0.0001$.

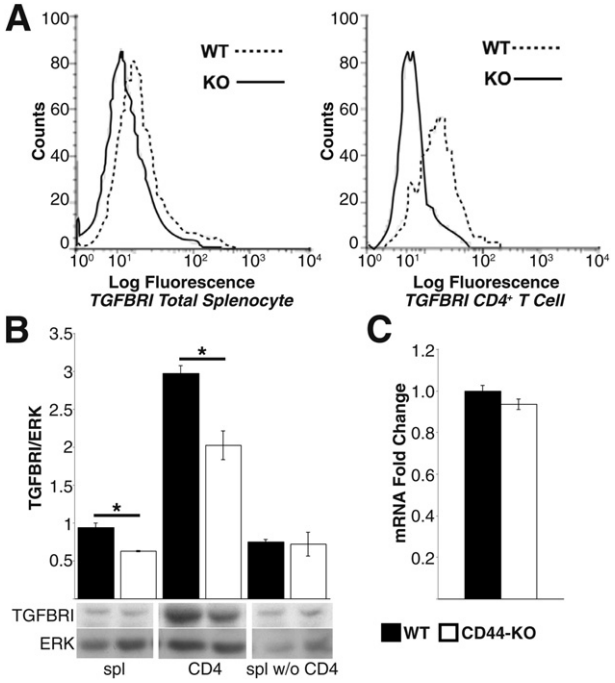

Figure 3 CD4 T cells from CD44-KO mice express lower surface and total TGFβRI protein despite similar amounts of mRNA. **A:** FACS analysis of total splenocytes (**left panel**) and $CD4^+$ T cells (**right panel**) for surface TGFβRI. Histograms are representative of two independent experiments, with combined $n = 8$. Median fluorescence intensity for CD4 T-cell TGFβRI: WT = 20.7 ± 3.2, and CD44-KO = 9.1 ± 0.4. $P = 0.006$. **B:** Western blot analysis of TGFβRI total protein expression in total splenocytes (spl), $CD4^+$ T cells (CD4), and splenocytes depleted of $CD4^+$ T cells (spl w/o CD4) (**top panel**) and densitometry quantification (**bottom panel**). Lysates were generated from three animals per strain. Data are expressed as ± SEM **C:** Real-time PCR quantification of TGFβRI from WT and CD44-KO $CD4^+$ T cells subject to ΔΔCt analysis. Data are expressed as means ± SEM, $n = 6$ per strain. $^*P = 0.05$, $^{**}P = 0.02$.

in the presence of HA, the best-characterized CD44 ligand. No statistically significant changes in Th17 polarization were observed in response to LMW or HMW HA treatment compared to culture in the absence of LMW or HMW HA (Figure 4B).

Increased EAE Severity Results from Loss of CD44 on BM-Derived and Stromal Cells

Because CD44 is ubiquitously expressed, we tested the possibility that CD44 expression on cells other than, or in addition to, circulating immune cells may also be important in EAE. To do so, BM-chimeric mice were generated by transfer of WT or CD44-KO BM into lethally irradiated WT or CD44-KO recipients. FACS analysis of CD44 expression in inguinal lymph node and splenic cells was used to determine the degree of chimerism in the lymphatic system of these mice. WT or CD44-KO mice that received WT BM (WT → WT and WT → KO, respectively) contained mostly WT immune cells ($CD45^+$, $CD44^+$), whereas WT or CD44-KO mice that received CD44-KO BM (KO → WT and KO → KO, respectively) contained mostly CD44-KO immune cells ($CD45^+$, $CD44^-$) (Figure 5, A–D). Further, FACS analysis of the microglial population ($CD11b^+$, $CD45^{lo}$) in the chimeric mice revealed that microglia from KO → WT and KO → KO chimeras lacked CD44 expression while WT → KO and WT → WT microglia expressed CD44 (Figure 5E). Thus, resident microglia were replaced by circulating donor cells following irradiation, as has been described previously.[43]

Next, EAE was examined in chimeric mice. As expected, and consistent with our previous experiments, the WT → WT mice had the least severe disease and lowest mortality rate, and the KO → KO mice had the highest disease severity and mortality rate. However, KO → WT mice and WT → KO mice both exhibited greater disease and mortality than WT → WT mice, and less disease and mortality than KO → KO mice (Figure 5, F–H, and Table 2). These data suggest that CD44 expression on both radiation-sensitive and -insensitive cells had an effect on disease severity. Further, though the surviving WT → KO mice had similar disease severity as the surviving KO → WT mice, the former showed a recovery that more closely followed the WT → WT chimeras, whereas the KO → WT had a lower overall mortality rate than the WT → KO group.

CD44-KO BrEC Support Enhanced T-Cell Adhesion and Transmigration

We investigated the possibility that loss of CD44 expression on radiation-insensitive EC of the blood vessels could result in increased T-cell adhesion or transendothelial migration, which could contribute to increased inflammation. Using WT and CD44-KO lymphocytes and low-passage immortalized murine BrEC, we examined the ability of resting or activated T cells to adhere to and transmigrate across quiescent or TNFα-stimulated BrEC monolayers. WT and CD44-KO BrEC both lacked P-selectin expression and expressed similar levels of adhesion molecules intercellular adhesion molecule 1 (ICAM-1), ICAM-2, vascular cell adhesion molecule (VCAM), and E-selectin (data not shown). Lymphocyte activation greatly facilitated adhesion, whereas TNFα stimulation of the BrEC appeared to be dispensable (Figure 6A). Therefore, only activated lymphocytes and unstimulated BrEC were used for the transmigration assays. There was significantly greater T-cell adhesion to, and migration across, the CD44-KO BrEC monolayer, compared to the WT BrEC monolayer, regardless of CD44 expression on the T cells (Figure 6, A and B).

Theoretically, lymphocyte adhesion can be affected by alterations in the endothelial glycocalyx, a network of membrane-bound glycoproteins and proteoglycans lining the endothelium luminally.[43,44] HA, typically anchored to EC by CD44, is a critical component of the glycocalyx. To identify the role of HA in adhesion in this system, we examined T-cell–EC adhesion following treatment of WT and CD44-KO EC with hyaluronidase (Figure 6C). Hyaluronidase treatment had no effect on lymphocyte (WT or CD44-KO) adhesion to WT EC. Although treatment of

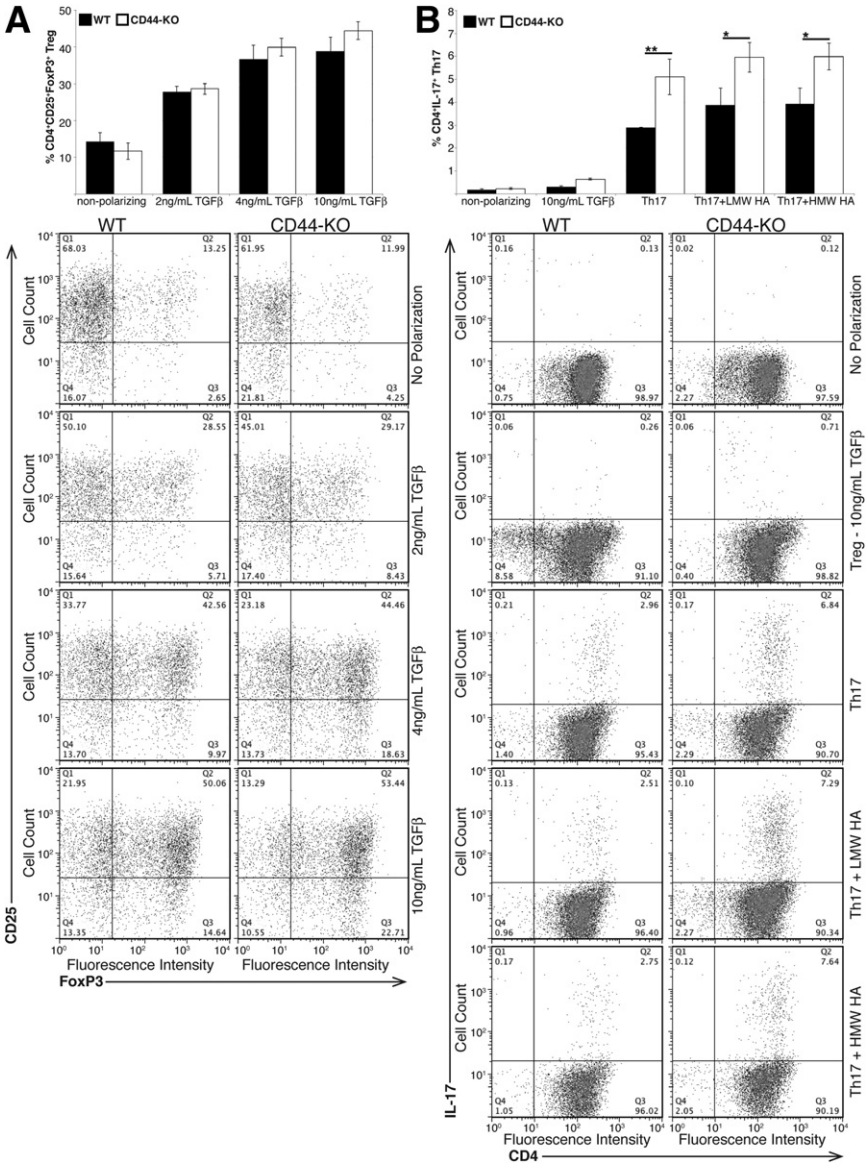

Figure 4 Naïve CD44-KO $CD4^+$ T cells have a similar capacity to polarize to the Treg phenotype, but have enhanced polarization to the Th17 phenotype as WT $CD4^+$ T cells *in vitro*. Equivalent numbers of naïve $CD4^+$ T cells were subjected to Treg (**A**) or Th17 (**B**) polarizing conditions *in vitro*. Polarization to these phenotypes was quantified via FACS analysis, and representative dot plots for each polarization are included below each graph. Data are representative of one of two (LMW/HMW HA Th17 conditions) or three (all other conditions) independent experiments with naïve $CD4^+$ T cells isolated from a total of six (LMW/HMW HA Th17 conditions) or nine (all other conditions) mice per strain and are expressed as means ± SEM. $*P \leq 0.05$, $**P \leq 0.02$.

CD44-KO EC monolayers with hyaluronidase reduced lymphocyte adhesion to levels observed on WT monolayers, we could not detect a difference in total HA abundance between WT and CD44-KO EC or spinal cords using immunohistochemistry (Supplemental Figure S2).

The CD44-KO Brain Vasculature Is More Permeable than WT in Naïve and Disease States

We next questioned whether there was differential BBB permeability in the CD44-KO mice, another endothelial defect that could promote increased inflammation. Intravenous injections of Evans Blue dye were used to assess vascular permeability of several vascular beds *in vivo*. In an unchallenged state, no permeability differences were observed in the inguinal lymph node blood vessels, dermal microvasculature, hepatic vasculature, or pulmonary vasculature. However, the cerebral vasculature of CD44-KO mice was significantly more permeable than in WT mice (Figure 7A). Immunostaining for IgG, which is larger than Evans Blue–bound albumin and is also excluded from EC junctions, further corroborated these results. The WT brain was devoid of IgG, whereas the CD44-KO brain had extensive IgG infiltration that localized to perivascular tissues (Figure 7B).

The integrity of the CNS vasculature was then assessed throughout EAE. The CD44-KO mice showed a sustained, though subtler, increase in permeability throughout the disease, which returned to baseline in the chronic stage of the disease (Figure 7C). During the course of EAE skin vessel permeability was unaffected, illustrating the specificity of the response.

We next examined the architecture of the different BBB structural components to identify the level at which the BBB is permeable in CD44-KO mice. Using immunofluorescence, we examined the localization of IgG in the brain of CD44-

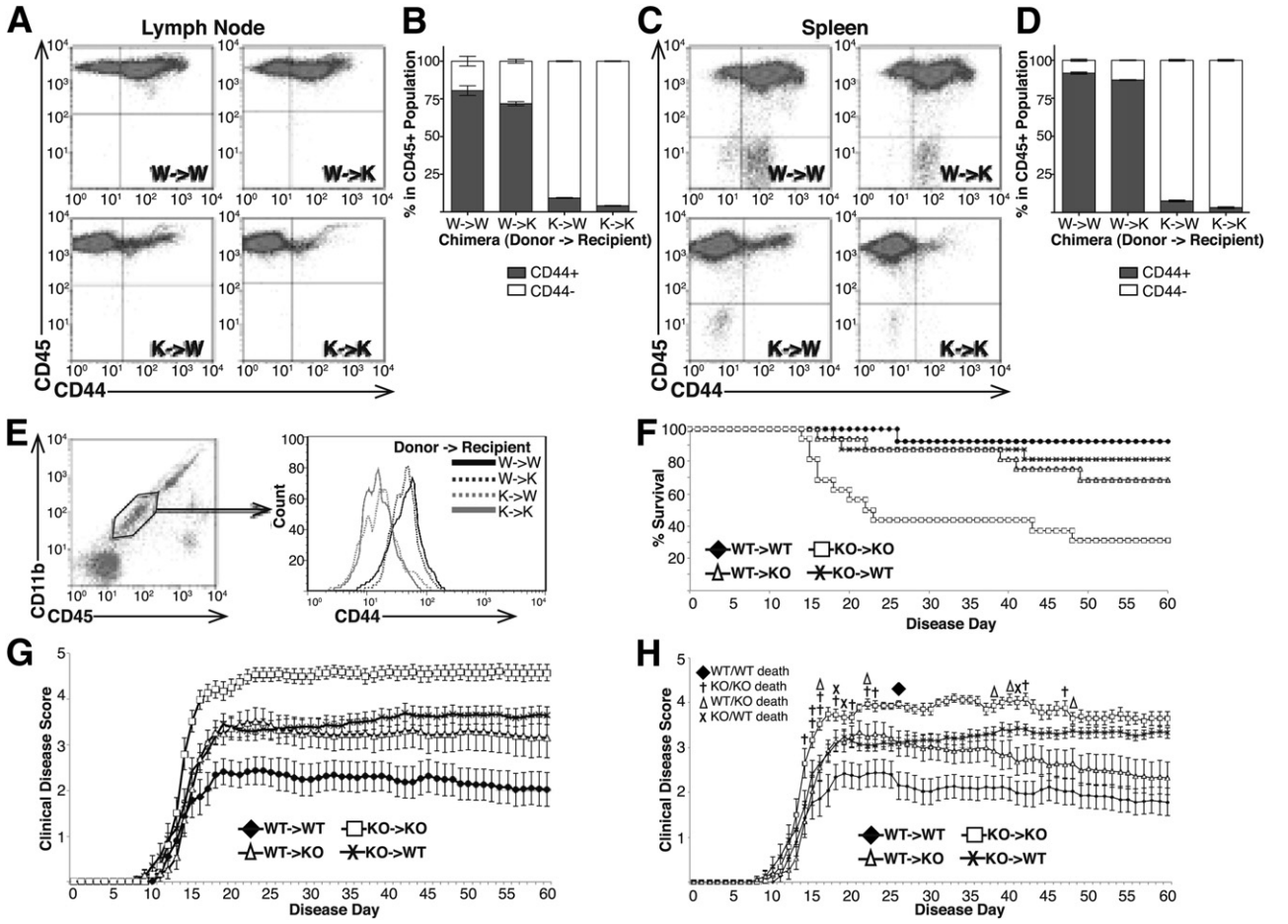

Figure 5 Increased EAE disease severity in CD44-KO mice is due to loss of CD44 on circulating and noncirculating cell types. BM chimeras were generated using WT or CD44-KO donor BM and WT or CD44-KO recipients, and subjected to EAE (BM donor→Recipient). **A** and **C**: Representative dot plots of FACS analysis of CD44 expression by immune cells ($CD45^+$cells) in inguinal lymph node cells (**A**) and splenic cells (**C**) from BM chimeric mice. **B** and **D**: Average percentage of $CD45^+$ cells expressing or lacking CD44 isolated from chimeric mouse inguinal lymph node (**B**) or spleen (**D**). Data are expressed as means ± SEM: $n = 4$ for each chimeric group. **E**: Microglia ($CD11b^+CD45^{lo}$) were isolated from BM-chimeric mice. Gated region represents the microglial population. Histograms represent CD44 expression within the microglial-gated population. **F**: Kaplan-Meier survival curve of chimeric animals throughout EAE. **G**: Clinical disease curve of chimeric animals with mortality scores included in average score from time of death throughout the remainder of the study. **H**: Clinical disease curve of chimeric animals with mortality scores included on day of death but excluded from average scores in subsequent days of study. Data are expressed as means ± SEM, from two independent experiments: $n = 16$ WT→WT; $n = 18$ all other groups.

KO mice with respect to EC marker CD31, endothelial basement membrane component collagen IV (ColIV), and astrocytic marker glial fibrillary acidic protein (GFAP). IgG was localized outside of EC CD31, but not astrocytic GFAP (Figure 7, D and E). In some vessels, IgG was found outside ColIV whereas in others, it appeared within the basement membrane to EC junctions, due to the punctate nature of IgG localization (Figure 7F).

Discussion

During EAE, autoreactive lymphocytes become activated and undergo differentiation in the periphery, migrate to the CNS, and interact with BrEC to exit the vasculature and gain access to the CNS parenchyma where they initiate inflammation and disease. Our data suggest that CD44 is involved in several of these processes as a negative regulator of inflammation with roles in CD4 T-cell differentiation, adhesion and transendothelial migration, and BBB permeability.

The proinflammatory phenotype of the CD44-KO mice is evidenced by increase in the following: clinical disease, immune and CD4 T-cell numbers within the CNS, antibody production, and a proinflammatory cytokine milieu. The similar kinetics of disease progression between the WT and CD44-KO suggests that the increased disease severity in the CD44-KO could result from altered CD4 T-cell differentiation, which could increase disease severity without affecting the disease time course. Despite similar cytokine production in naïve animals, and similar CD4 T-cell numbers and activation states ($CD62L^+$ and $CD69^+$) in the periphery of immunized animals, the phenotypic profile of CD4 T cells was markedly different between the two strains following disease induction.

Increased IL-17 production by CD44-KO splenocytes during EAE strongly indicated greater quantities of Th17 cells,

Table 2 BM Chimera EAE Clinical Disease Characteristics

Donor listed first, recipient second	Average day disease onset	Average maximum disease score	Sum daily average disease score	Disease index	Percent mortality
WT → WT	13.92	2.73†††	105.2	755.6†††	7.00
CD44-KO → WT	12.88	4.09**††	163.9	1273.3**††	18.75
WT → CD44-KO	13.67	3.80*†	151.2	1106.7*††	31.25
CD44-KO → CD44-KO	12.06	4.75***	212.2	1758.69***	68.75

EAE disease measurements from BM chimeric mice.
*$P < 0.05$, **$P < 0.005$, and ***$P < 0.0001$ versus WT → WT.
$^{\dagger}P < 0.006$, $^{\dagger\dagger}P < 0.0004$, and $^{\dagger\dagger\dagger}P < 0.0001$ versus KO → KO.

because IL-17 is predominantly a CD4 T-cell product.[8,45] Further, the significantly increased levels of IL-6 and IL-23, though possibly produced by multiple cell types, also support an increase in the Th17 population, because these cytokines are required for Th17 maturation. Moreover, the trend for increased IFN-γ production in the CD44-KO mice further illustrates an augmented proinflammatory environment in the CD44-KO despite similar levels of IL-10 and TGF-β, both of which have pro- and anti-inflammatory functions in the immune system.[46,47] These data are consistent with a proinflammatory environment skewed toward Th17-associated cytokine milieu in the CD44-KO mice.

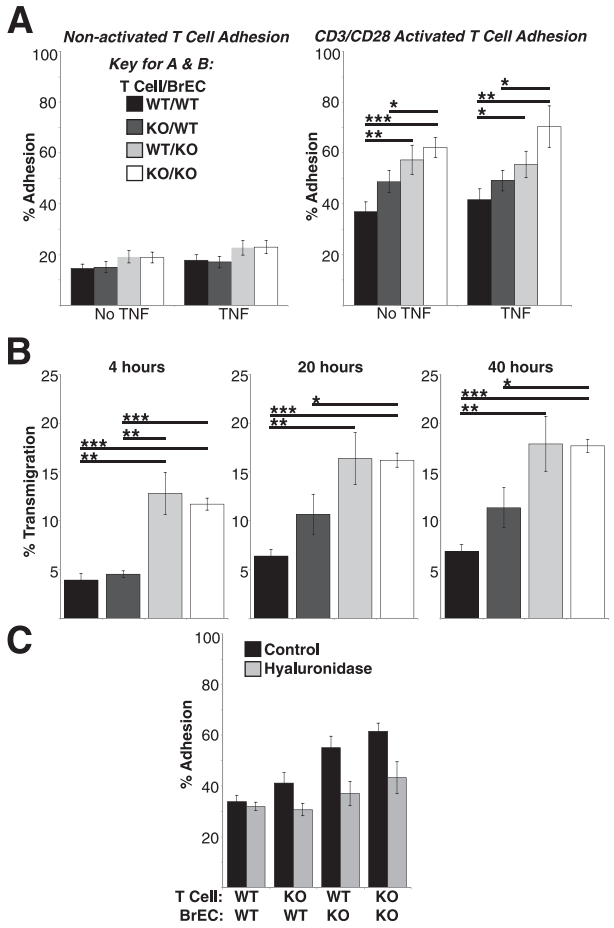

Figure 6 CD44-KO BrEC monolayers support greater adhesion and transmigration than do WT BrEC, regardless of T-cell expression of CD44. **A:** Adhesion of nonactivated and polyclonally activated T cells to unstimulated and TNFα-stimulated WT and CD44-KO confluent BrEC monolayers. **B:** Transmigration of polyclonally activated T cells through confluent WT and CD44-KO BrEC monolayers in the Transwell system. **C:** Adhesion of polyclonally activated T cells to unstimulated BrEC monolayers with and without hyaluronidase treatment. *$P \leq 0.05$, **$P \leq 0.007$, and ***$P \leq 0.0001$. Average data are presented as means ± SEM from three independent experiments, $n = 9$ for each condition.

Tregs control various aspects of the immune response, including limiting activation and function of innate and adaptive immune cells.[48] Therefore, Tregs are critical mediators of EAE; Tregs are involved not only in limiting inflammation within the CNS, but also play a critical suppressive role during priming in the peripheral compartment. Further, peripheral Tregs from MS patients show a decreased suppressive capacity.[49] It is plausible that the increased CNS inflammation, antibody production, and proinflammatory cytokine production observed in the CD44-KO mice are a result of defective immunosuppression by Tregs in the peripheral compartment. We found reduced numbers of Tregs in the periphery of CD44-KO mice throughout the disease, and although we did not examine Treg suppressive function, previous studies have shown that CD44 expression correlates with superior Treg suppressive function in both murine and human cells.[50,51] Therefore, overall suppression of inflammation during EAE could be impaired, not only by a reduced number of Tregs, but also by reduced Treg function in the CD44-KO mouse.

Though there are fewer Tregs in the CD44-KO spleen following EAE induction, these mice have similar numbers of naturally occurring Tregs in the naïve state as WT mice. Thus, the reduced Treg population observed throughout the disease is likely a consequence of defective generation or survival of iTregs. Moreover, an increase in Th17 cells accompanies the reduction of Tregs in the CD44-KO throughout the disease. These cell types share a common developmental pathway, as both require TGF-β for differentiation, but use different downstream signaling components to achieve their different phenotypic programs.[52] Th17 differentiation is favored at lower TGF-β concentrations, whereas Treg differentiation is favored at higher concentrations.[53] Conceivably, the decreased TGFβRI expression on CD44-KO CD4 T cells attenuates the TGF-β signal, or alters the ratio of TGFβRI with other receptors, either of which could result in differential downstream signaling and altered polarization. *In vitro*,

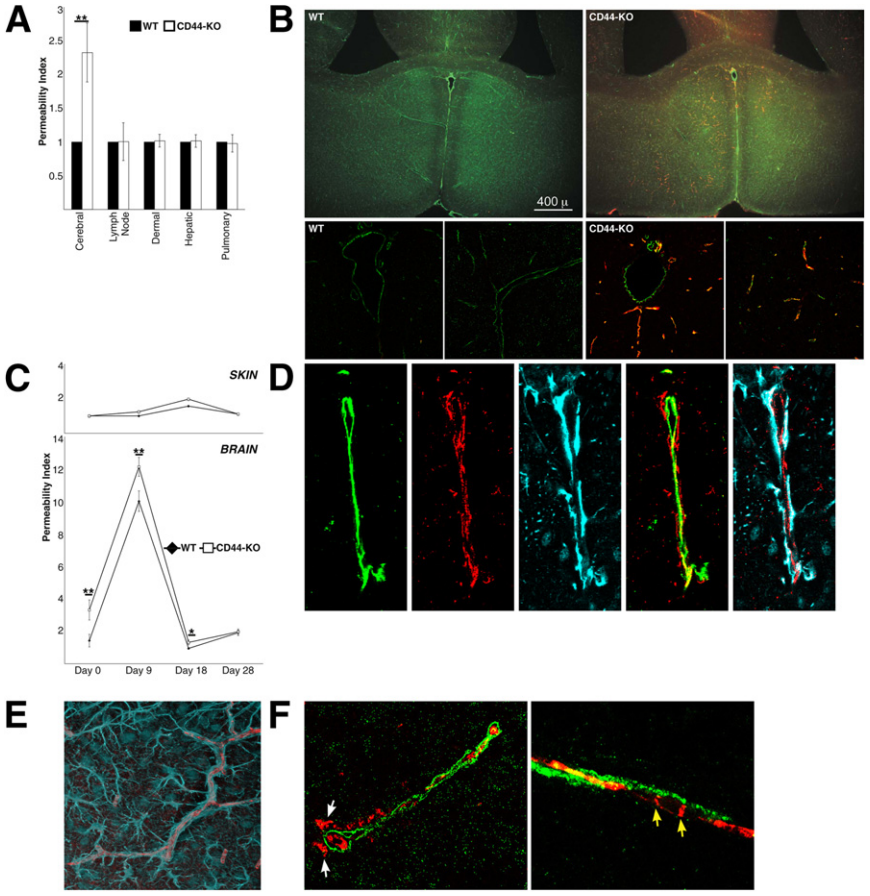

Figure 7 The CD44-KO BBB is partially disrupted because the cerebral vasculature, but not the astrocytic component, of the CD44-KO is significantly more permeable than WT to albumin and IgG before and following immunization. **A:** Baseline permeability was determined using Evans Blue dye. For each vascular bed, WT permeability indices were set equal to one, and CD44-KO indices were calculated relative to WT values. Data are expressed as means ± SEM. **B:** Immunofluorescent images of vascular marker CD31 (green) and murine IgG (red) in naïve WT and CD44-KO brain. **Top row,** representative low-power images (×4 magnification); **bottom row,** representative high-power images (×63 magnification) derived using confocal microscopy. Images are representative of three independent experiments. **C:** Evans Blue permeability index in cerebral (**lower panel**) and dermal (**upper panel**) vasculature post-EAE induction. Six animals were used per strain, per disease day. Data are expressed as means ± SEM. $*P \leq 0.05$, $**P < 0.03$. **D**—**F:** Representative high-power (×63 magnification) confocal immunofluorescent images of three independent experiments in naïve CD44-KO brain. **D:** From left to right: CD31 (green), IgG (red), and astrocytic marker GFAP (cyan) in vessel cross section. **Second-to-last image** is the merger of CD31 and IgG, and the **right-most image** is the merger of GFAP and IgG. **E:** Longitudinal vessel brain vessel section; GFAP (cyan), IgG (red) immunofluorescence. **F:** Cross (**left panel**) and longitudinal (**right panel**) vessel sections for basement membrane component collagen IV (green) and IgG (red). **White arrows** indicate IgG localization outside collagen IV; **yellow arrows** indicate IgG localized to endothelial junctions.

naïve WT and CD44-KO CD4 T cells demonstrate an equivalent polarization to Tregs in response to TGF-β, but CD44-KO CD4 T cells have enhanced polarization to the Th17 phenotype (which might have been greater if IL-23 had been administered sequentially instead of simultaneously[8]). Despite their common developmental pathway, Th17 and Treg fates are mutually exclusive, and cytokines produced by one inhibit, or even reverse, differentiation into the other.[8,46] As such, it is possible that altered TGF-β signaling in the CD44-KO tips the balance of T-cell differentiation toward Th17, which in turn inhibits further iTreg generation, resulting in lower Treg numbers and a Th17-skewed profile *in vivo*. The reverse can also be true, where decreases in Th17 cells are met with reciprocal increases in Treg, resulting in an amelioration of EAE.[54]

Altered glycogen synthase kinase 3β (GSK3β) activation and signaling could also be a contributing factor to enhanced Th17 differentiation in CD44-KO T cells. Recently, inhibition of GSK3β was shown to prevent *in vitro* Th17 differentiation.[55] GSK3β is required for signal transducer and activator of transcription 3 (STAT3) activation[55] and also promotes degradation of SMAD family member 3 (Smad3) in the absence of TGF-β.[56] Because STAT3 is required for Th17 differentiation, whereas Smad3 inhibits this process, it is likely that both actions of GSK3β contribute to the generation of Th17 cells. Interestingly, we have found increased activation of GSK3β in CD44-KO EC (unpublished data). Further, changes in GSK3β activation could be related to alterations in TGF-β signaling, as there is crosstalk between these signaling pathways.[57,58] In fact, TGF-β signaling can lead to inactivation of GSK3β.[57] In the CD44-KO T cells, a plausible model could be that differential TGF-β signaling, in the presence of appropriate cytokines, leads to increased GSK3β activation, which then promotes increased Smad3 degradation and STAT3 activation, resulting in enhanced Th17 differentiation. Further, GSK3β activation is not observed in response to TGF-β alone or in iTregs.[55] If GSK3β-dependent mechanisms are responsible for altered Th17 generation in CD44-KO cells, this could explain why no differences in iTreg polarization are observed *in vitro*, whereas decreased iTreg generation *in vivo* results from the increased numbers of Th17 cells. Finally, active GSK3β is also required for inflammatory cell production of IL-6.[55,59] IL-6 is produced by innate immune cells and Th17 cells, inhibits iTreg differentiation, and is produced in greater quantities in CD44-KO splenocytes following MOG_{35-55} stimulation. If GSK3β is indeed increased in CD44-KO cells, this could be a potential explanation for the increased IL-6 production as well.

It is a novel finding that CD44 regulates TGFβRI expression. Our data suggest that this regulation in CD4 T cells occurs at the posttranscriptional level. Possibly, CD44 could aid in stabilization of TGFβRI at the plasma membrane,

potentially through direct physical interaction, which has been previously demonstrated in metastatic breast tumor cells.[60] Further, binding of HA to CD44 led to Smad3 activation, a downstream component in TGF-β signaling, which is of particular interest because Smad3 inhibits Th17 differentiation.[52] This introduces the possibility that the potentially altered TGF-β signaling in the CD44-KO could be a result, not only of decreased TGFβRI, but also or alternatively, of loss of interaction between CD44 and TGFβRI.

Our BM-chimeric EAE data illustrated that increased EAE disease severity in the CD44-KO mice is due to loss of CD44 on both BM-derived and non−BM-derived cell types, because any chimeric mice with both WT and CD44-KO components showed intermediate disease severity compared to those with only WT or CD44-KO components. It is interesting that the WT mice receiving CD44-KO BM (KO → WT) showed a chronic persistence of disease symptoms, whereas the CD44-KO mice that received WT BM (WT → KO) elicited a recovery, despite similar maximal disease severity between these two chimeras. Conceivably, the former experiences greater disease than a WT → WT chimera because they contain CD44-KO T cells, and as such, experience the same alterations in CD4 T-cell profiles, namely increased numbers of Th17 cells and decreased numbers of Tregs. As Tregs are involved in promoting resolution of EAE,[12] as well as limiting the inflammatory response, mice with reduced numbers of Tregs, such as those with CD44-KO T cells, would likely fail to exhibit disease recovery as well as having greater clinical symptoms. The KO mice receiving WT BM (WT → KO) by contrast contain a CD44-KO BBB, and as such, experience increased BBB permeability, which may allow greater quantities of immune cells to penetrate the CNS, resulting in greater inflammation and disease, but maintain sufficient Tregs to elicit better recovery. The combination of altered T-cell differentiation and increased BBB permeability would likely result in the greatest disease, which is observed in the KO → KO chimeric mice.

Though there are multiple potential noncirculating cells types involved in EAE, including lymph node stromal cells and CNS resident cells, we directed our focus on vascular EC due to the crucial role of the vasculature in promoting and limiting inflammatory processes. Endothelial loss of CD44 promoted enhanced adhesion and migration of T cells *in vitro*, because CD44-KO BrEC monolayers support greater adhesion and transmigration than do WT BrEC monolayers, regardless of T-cell expression of CD44. *In vivo*, increased adhesion and transendothelial transmigration can in turn lead to increased immune cell extravasation into the CNS parenchyma and a subsequent increase in CNS inflammation. Classical adhesion molecules, such as ICAM and VCAM, are likely not the cause for increased adhesion, as CD44-KO BrEC express similar levels of these molecules in the absence of TNFα. Though TNFα stimulation increases expression of these molecules, we did not observe increased adhesion in response to TNFα in either cell type.

Theoretically, increased adhesion could result from modifications to the endothelial glycocalyx, a network of membrane-bound glycoproteins and proteoglycans lining the endothelium luminally.[43,44] HA, which can be anchored by CD44, is a critical component of the glycocalyx, and due to its length, is the only glucosaminoglycan capable of forming entangled networks.[61] Consequently, loss of HA from the EC surface could result in decreased depth of this layer, rendering other adhesive molecules more accessible, leading to greater lymphocytic adhesion. Alternatively, increased HA levels could also form a thicker, tangled, stickier mesh, allowing easier entrapment of lymphocytes. To our surprise, we found no effect of hyaluronidase treatment on lymphocyte adhesion to WT EC. Even more surprising, treatment of CD44-KO EC monolayers with hyaluronidase reduced lymphocyte adhesion to the levels observed on WT monolayers. This suggests that HA is a contributing factor in the increased lymphocyte adhesion in the absence of HA receptor CD44. One potential explanation is that in the absence of CD44, EC use alternative or compensatory HA receptors, such as receptor for hyaluronic acid-mediated motility (RHAMM), to tether HA to the EC surface. In doing so, this could alter HA conformation or signaling, arrangement and organization of the endothelial surface layer, and regulation of cellular processes and behaviors. For example, in collagen-induced arthritic CD44-KO mice, cell migration and up-regulation of inflammatory genes occurred via signaling through the RHAMM pathway.[32] It is also possible that loss of CD44 leads HA accumulation, because CD44 is the most common endocytic receptor for HA responsible for HA turnover. Animals with conditional loss of CD44 within the dermis overaccumulated HA in this tissue.[62] Increased endothelial HA accumulation could lead to a more adhesive endothelial glycocalyx. However, immunohistochemical analysis revealed similar levels of total HA in WT and CD44-KO spinal cord vessels and BrEC (Supplemental Figure S2). Although no differences were identified in total HA expression, immunohistochemistry is incapable of distinguishing between abundance of HMW or LMW HA fragments, or between differential molecular interactions or conformations, both of which may be involved in adhesive events.

It remains possible that a differential molecular and electrostatic composition of the endothelial surface layer may contribute to increased lymphocytic adhesion. Many post-translational modifications of CD44 produce negative charges, and loss of CD44 could result in loss of electrostatic charge repulsion between cells, resulting in greater adhesion. However, further manipulation of the complex organization of the endothelial surface layer was beyond the scope of this study. Additionally, changes in endothelial chemokine production could also affect lymphocyte-EC adhesion.[63]

Enhanced transendothelial migration can result from increased T-cell−EC adhesive interactions, decreased junctional competency between EC,[64] or increased protease[64] or chemokine production.[63] CD44 could participate in one or more of these processes, some of which are currently under

investigation in our laboratory. Increased permeability of the CD44-KO BBB, suggesting loss of EC junctional competency, is at least one potential explanation for enhanced transmigration. Further, CD44 has previously established roles in matrix metalloproteinase (MMP) biology,[65,66] which are known to affect vascular permeability.[67] Previous studies from our laboratory have shown that dysregulation of BBB permeability and MMP expression can lead to enhanced lymphocyte transmigration and increased EAE severity.[41,68]

During the pathogenesis of EAE, the BBB is compromised and becomes permeable to plasma proteins and immune cells. Increased BBB permeability, such as that in CD44-KO, would allow for intensification of these processes and increased inflammation. The inherent leakiness in the naïve CD44-KO BBB is likely even further exacerbated throughout the disease by inflammatory cytokines, such as IL-17, which enhance BBB permeability and are produced in greater amounts in the CD44-KO.

The inherent partial disruption of BBB integrity in unimmunized CD44-KO mice is a particularly fascinating finding. The BBB is a dynamic functional and structural component of the CNS, charged with the imperative task of maintaining an appropriate CNS microenvironment.[69] This barrier is formed primarily by highly specialized EC, surrounded by a complex basement membrane, invested by pericytes, and ensheathed by astrocytic end-foot processes. A complex crosstalk between glia, pericytes, BrEC, and their extracellular matrices is critical for formation and maintenance of BBB integrity and function. Thus, CD44 expression on multiple BBB cell types could affect the way these components interact with one another and/or their underlying extracellular matrix, leading to a disruption of the appropriate intercellular communication necessary for junctional integrity in the brain vasculature. This could result from changes in direct contact between these cell types, or altered expression of secreted molecules, such as MMPs, from one or more of these cells. CD44, through its numerous potential molecular interactions, has the capacity to affect both in a myriad of ways. Though the exact mechanism of BBB regulation by CD44 is beyond the scope of the current study, these data have illustrated that EC junctions are disrupted in the CD44-KO BBB. Though IgG localizes outside the endothelial elements in the CD44-KO brain, its localization within astrocytic processes suggests it does not penetrate beyond the astrocytic component. It is unclear how or why IgG does not permeate beyond the astrocytic end feet in the CD44-KO brain. However, it is clear that CD44 expression on BBB cells is required to maintain EC junctional, and thus BBB, integrity. Loss of EC junctional competency results from loss of molecular cohesion at the EC border, subsequent to decreased adhesive interactions between junctional molecules, or increased barrier-disrupting agents, such as proteases, that cleave junctional bonds directly or disrupt the underlying matrix that supports the maintenance of these interactions. These processes are dependent on the complex molecular crosstalk between BBB components and can be regulated by CD44 interactions in various ways as described above. Additionally, these findings may have important implications in future BBB permeability studies. Permeability needs to be assessed on various levels because permeability of one, but not all, levels of the BBB could result in different biological consequences, and not all assays are capable of distinguishing between total and partial barrier disruption.

It is also important to note that we cannot conclude increased leakage of Evans Blue into the CNS relative to other tissues, but only in the CD44-KO CNS compared to the WT CNS. Using Evans Blue, it is not possible to compare permeability of one organ to another. Because the dye is extracted in formamide, and parenchymal beds have differential compositions, the resulting turbidity differences between organ samples cause skewed spectrophotometric absorbance values. For example, myelin within the CNS causes relatively higher turbidity and absorbance values than vascular beds such as the skin that lack such components.

Our findings that CD44 acts as a negative regulator of inflammation in EAE are consistent with increased inflammation observed in various experimental models in CD44-deficient mice. While the current study was underway, Guan et al[42] reported that CD44-KO mice showed diminished EAE severity that correlated with more anti-inflammatory CD4 T-cell profiles and differentiation *in vivo* and *in vitro*. The reasons for the discrepancies between Guan et al[42] and our work are unclear. In an attempt to understand these differences, we used several EAE induction protocols, including that of Guan et al, and have found in all circumstances that the CD44-KO mice succumb to more severe disease than do WT mice (Supplemental Figure S1 and Supplemental Table S1). Further, though these data are derived from mice from the Jackson Laboratory, we observed similar disease progression in a separate and independently derived CD44-KO strain that was a gift from Dr. Paul W. Noble[25,27] (Supplemental Figure S1 and Supplemental Table S1).

Conclusions

In summary, CD44 is a complex multifunctional molecule that can differentially regulate various cellular processes depending on cell type, isoform expression, posttranslational modification, and interacting ligand. Here, we have identified several mechanisms of EAE that are altered in the absence of CD44, leading to exacerbated disease. Mechanistic understanding of how CD44 alters each process is still under investigation and must take into consideration the heterogeneity of the CD44 family. Nonetheless, our data from CD44-deficient mice illustrate a role for CD44 in limiting inflammation in EAE through several mechanisms that might be applied to other immune diseases as well. Specifically, we have identified novel roles for CD44 in regulating the CD4 T-cell expression of TGFβRI, CD4 T-cell differentiation, and BBB integrity.

Acknowledgments

We thank Dr. Nancy Ruddle for her critical reading of this manuscript and Dr. Michael Centrella for generously providing antibodies to TGF-β receptors.

Supplemental Data

Supplemental material for this article can be found at *http://dx.doi.org/10.1016/j.ajpath.2013.01.003*.

References

1. Steinman L, Zamvil SS: How to successfully apply animal studies in experimental allergic encephalomyelitis to research on multiple sclerosis. Ann Neurol 2006, 60:12−21
2. Goverman J: Autoimmune T cell responses in the central nervous system. Nat Rev Immunol 2009, 9:393−407
3. Oliver AR, Lyon GM, Ruddle NH: Rat and human myelin oligodendrocyte glycoproteins induce experimental autoimmune encephalomyelitis by different mechanisms in C57BL/6 mice. J Immunol 2003, 171:462−468
4. O'Brien K, Fitzgerald DC, Naiken K, Alugupalli KR, Rostami AM, Gran B: Role of the innate immune system in autoimmune inflammatory demyelination. Curr Med Chem 2008, 15:1105−1115
5. Reboldi A, Coisne C, Baumjohann D, Benvenuto F, Bottinelli D, Lira S, Uccelli A, Lanzavecchia A, Engelhardt B, Sallusto F: C-C chemokine receptor 6-regulated entry of TH-17 cells into the CNS through the choroid plexus is required for the initiation of EAE. Nat Immunol 2009, 10:514−523
6. Kebir H, Kreymborg K, Ifergan I, Dodelet-Devillers A, Cayrol R, Bernard M, Giuliani F, Arbour N, Becher B, Prat A: Human TH17 lymphocytes promote blood-brain barrier disruption and central nervous system inflammation. Nat Med 2007, 13:1173−1175
7. Hofstetter H, Gold R, Hartung HP: Th17 cells in MS and experimental autoimmune encephalomyelitis. Int MS J 2009, 16:12−18
8. Bettelli E, Carrier Y, Gao W, Korn T, Strom TB, Oukka M, Weiner HL, Kuchroo VK: Reciprocal developmental pathways for the generation of pathogenic effector TH17 and regulatory T cells. Nature 2006, 441:235−238
9. Mangan PR, Harrington LE, O'Quinn DB, Helms WS, Bullard DC, Elson CO, Hatton RD, Wahl SM, Schoeb TR, Weaver CT: Transforming growth factor-beta induces development of the T(H)17 lineage. Nature 2006, 441:231−234
10. Huppert J, Closhen D, Croxford A, White R, Kulig P, Pietrowski E, Bechmann I, Becher B, Luhmann HJ, Waisman A, Kuhlmann CR: Cellular mechanisms of IL-17-induced blood-brain barrier disruption. FASEB J 2010, 24:1023−1034
11. Zhang X, Koldzic DN, Izikson L, Reddy J, Nazareno RF, Sakaguchi S, Kuchroo VK, Weiner HL: IL-10 is involved in the suppression of experimental autoimmune encephalomyelitis by CD25+CD4+ regulatory T cells. Int Immunol 2004, 16:249−256
12. McGeachy MJ, Stephens LA, Anderton SM: Natural recovery and protection from autoimmune encephalomyelitis: contribution of CD4+CD25+ regulatory cells within the central nervous system. J Immunol 2005, 175:3025−3032
13. Chen W, Jin W, Hardegen N, Lei KJ, Li L, Marinos N, McGrady G, Wahl SM: Conversion of peripheral CD4+CD25- naive T cells to CD4+CD25+ regulatory T cells by TGF-beta induction of transcription factor Foxp3. J Exp Med 2003, 198:1875−1886
14. Bluestone JA, Abbas AK: Natural versus adaptive regulatory T cells. Nat Rev Immunol 2003, 3:253−257
15. Bennett J, Basivireddy J, Kollar A, Biron KE, Reickmann P, Jefferies WA, McQuaid S: Blood-brain barrier disruption and enhanced vascular permeability in the multiple sclerosis model EAE. J Neuroimmunol 2010, 229:180−191
16. Minagar A, Alexander JS: Blood-brain barrier disruption in multiple sclerosis. Mult Scler 2003, 9:540−549
17. Thorne RF, Legg JW, Isacke CM: The role of the CD44 transmembrane and cytoplasmic domains in co-ordinating adhesive and signalling events. J Cell Sci 2004, 117:373−380
18. Ponta H, Sherman L, Herrlich PA: CD44: from adhesion molecules to signalling regulators. Nat Rev Mol Cell Biol 2003, 4:33−45
19. DeGrendele HC, Estess P, Siegelman MH: Requirement for CD44 in activated T cell extravasation into an inflammatory site. Science 1997, 278:672−675
20. Nedvetzki S, Walmsley M, Alpert E, Williams RO, Feldmann M, Naor D: CD44 involvement in experimental collagen-induced arthritis (CIA). J Autoimmun 1999, 13:39−47
21. Mikecz K, Brennan FR, Kim JH, Glant TT: Anti-CD44 treatment abrogates tissue oedema and leukocyte infiltration in murine arthritis. Nat Med 1995, 1:558−563
22. Weiss L, Slavin S, Reich S, Cohen P, Shuster S, Stern R, Kaganovsky E, Okon E, Rubinstein AM, Naor D: Induction of resistance to diabetes in non-obese diabetic mice by targeting CD44 with a specific monoclonal antibody. Proc Natl Acad Sci U S A 2000, 97: 285−290
23. Katoh S, Ishii N, Nobumoto A, Takeshita K, Dai SY, Shinonaga R, Niki T, Nishi N, Tominaga A, Yamauchi A, Hirashima M: Galectin-9 inhibits CD44-hyaluronan interaction and suppresses a murine model of allergic asthma. Am J Respir Crit Care Med 2007, 176: 27−35
24. Brocke S, Piercy C, Steinman L, Weissman IL, Veromaa T: Antibodies to CD44 and integrin alpha4, but not L-selectin, prevent central nervous system inflammation and experimental encephalomyelitis by blocking secondary leukocyte recruitment. Proc Natl Acad Sci U S A 1999, 96:6896−6901
25. Teder P, Vandivier RW, Jiang D, Liang J, Cohn L, Pure E, Henson PM, Noble PW: Resolution of lung inflammation by CD44. Science 2002, 296:155−158
26. Wang Q, Teder P, Judd NP, Noble PW, Doerschuk CM: CD44 deficiency leads to enhanced neutrophil migration and lung injury in Escherichia coli pneumonia in mice. Am J Pathol 2002, 161: 2219−2228
27. Liang J, Jiang D, Griffith J, Yu S, Fan J, Zhao X, Bucala R, Noble PW: CD44 is a negative regulator of acute pulmonary inflammation and lipopolysaccharide-TLR signaling in mouse macrophages. J Immunol 2007, 178:2469−2475
28. van der Windt GJ, van 't Veer C, Florquin S, van der Poll T: CD44 deficiency is associated with enhanced Escherichia coli-induced proinflammatory cytokine and chemokine release by peritoneal macrophages. Infect Immun 2010, 78:115−124
29. Muto J, Yamasaki K, Taylor KR, Gallo RL: Engagement of CD44 by hyaluronan suppresses TLR4 signaling and the septic response to LPS. Mol Immunol 2009, 47:449−456
30. Huebener P, Abou-Khamis T, Zymek P, Bujak M, Ying X, Chatila K, Haudek S, Thakker G, Frangogiannis NG: CD44 is critically involved in infarct healing by regulating the inflammatory and fibrotic response. J Immunol 2008, 180:2625−2633
31. McKallip RJ, Fisher M, Gunthert U, Szakal AK, Nagarkatti PS, Nagarkatti M: Role of CD44 and its v7 isoform in staphylococcal enterotoxin B-induced toxic shock: cD44 deficiency on hepatic mononuclear cells leads to reduced activation-induced apoptosis that results in increased liver damage. Infect Immun 2005, 73: 50−61
32. Nedvetzki S, Gonen E, Assayag N, Reich R, Williams RO, Thurmond RL, Huang JF, Neudecker BA, Wang FS, Turley EA, Naor D: RHAMM, a receptor for hyaluronan-mediated motility, compensates for CD44 in inflamed CD44-knockout mice: a different

interpretation of redundancy. Proc Natl Acad Sci U S A 2004, 101: 18081–18086
33. Hutas G, Bajnok E, Gal I, Finnegan A, Glant TT, Mikecz K: CD44-specific antibody treatment and CD44 deficiency exert distinct effects on leukocyte recruitment in experimental arthritis. Blood 2008, 112:4999–5006
34. Girgrah N, Letarte M, Becker LE, Cruz TF, Theriault E, Moscarello MA: Localization of the CD44 glycoprotein to fibrous astrocytes in normal white matter and to reactive astrocytes in active lesions in multiple sclerosis. J Neuropathol Exp Neurol 1991, 50:779–792
35. Back SA, Tuohy TM, Chen H, Wallingford N, Craig A, Struve J, Luo NL, Banine F, Liu Y, Chang A, Trapp BD, Bebo BF Jr, Rao MS, Sherman LS: Hyaluronan accumulates in demyelinated lesions and inhibits oligodendrocyte progenitor maturation. Nat Med 2005, 11: 966–972
36. Knudson W, Chow G, Knudson CB: CD44-mediated uptake and degradation of hyaluronan. Matrix Biol 2002, 21:15–23
37. Noble PW: Hyaluronan and its catabolic products in tissue injury and repair. Matrix Biol 2002, 21:25–29
38. Pinter E, Barreuther M, Lu T, Imhof BA, Madri JA: Platelet-endothelial cell adhesion molecule-1 (PECAM-1/CD31) tyrosine phosphorylation state changes during vasculogenesis in the murine conceptus. Am J Pathol 1997, 150:1523–1530
39. Cardona AE, Huang D, Sasse ME, Ransohoff RM: Isolation of murine microglial cells for RNA analysis or flow cytometry. Nat Protoc 2006, 1:1947–1951
40. Graesser D, Mahooti S, Haas T, Davis S, Clark RB, Madri JA: The interrelationship of alpha4 integrin and matrix metalloproteinase-2 in the pathogenesis of experimental autoimmune encephalomyelitis. Lab Invest 1998, 78:1445–1458
41. Graesser D, Solowiej A, Bruckner M, Osterweil E, Juedes A, Davis S, Ruddle NH, Engelhardt B, Madri JA: Altered vascular permeability and early onset of experimental autoimmune encephalomyelitis in PECAM-1-deficient mice. J Clin Invest 2002, 109: 383–392
42. Guan H, Nagarkatti PS, Nagarkatti M: CD44 reciprocally regulates the differentiation of encephalitogenic Th1/Th17 and Th2/regulatory T cells through epigenetic modulation involving DNA methylation of cytokine gene promoters, thereby controlling the development of experimental autoimmune encephalomyelitis. J Immunol 2011, 186: 6955–6964
43. Reitsma S, Slaaf DW, Vink H, van Zandvoort MA, oude Egbrink MG: The endothelial glycocalyx: composition, functions, and visualization. Pflugers Arch 2007, 454:345–359
44. Nandi A, Estess P, Siegelman MH: Hyaluronan anchoring and regulation on the surface of vascular endothelial cells is mediated through the functionally active form of CD44. J Biol Chem 2000, 275: 14939–14948
45. Fossiez F, Djossou O, Chomarat P, Flores-Romo L, Ait-Yahia S, Maat C, Pin JJ, Garrone P, Garcia E, Saeland S, Blanchard D, Gaillard C, Das Mahapatra B, Rouvier E, Golstein P, Banchereau J, Lebecque S: T cell interleukin-17 induces stromal cells to produce proinflammatory and hematopoietic cytokines. J Exp Med 1996, 183: 2593–2603
46. Li MO, Flavell RA: TGF-beta: a master of all T cell trades. Cell 2008, 134:392–404
47. Sanjabi S, Zenewicz LA, Kamanaka M, Flavell RA: Anti-inflammatory and pro-inflammatory roles of TGF-beta, IL-10, and IL-22 in immunity and autoimmunity. Curr Opin Pharmacol 2009, 9:447–453
48. Shevach EM: Mechanisms of foxp3+ T regulatory cell-mediated suppression. Immunity 2009, 30:636–645
49. O'Connor RA, Anderton SM: Foxp3+ regulatory T cells in the control of experimental CNS autoimmune disease. J Neuroimmunol 2008, 193:1–11
50. Firan M, Dhillon S, Estess P, Siegelman MH: Suppressor activity and potency among regulatory T cells is discriminated by functionally active CD44. Blood 2006, 107:619–627
51. Bollyky PL, Falk BA, Long SA, Preisinger A, Braun KR, Wu RP, Evanko SP, Buckner JH, Wight TN, Nepom GT: CD44 costimulation promotes FoxP3+ regulatory T cell persistence and function via production of IL-2, IL-10, and TGF-beta. J Immunol 2009, 183: 2232–2241
52. Martinez GJ, Zhang Z, Chung Y, Reynolds JM, Lin X, Jetten AM, Feng XH, Dong C: Smad3 differentially regulates the induction of regulatory and inflammatory T cell differentiation. J Biol Chem 2009, 284:35283–35286
53. Zhou L, Lopes JE, Chong MM, Ivanov II, Min R, Victora GD, Shen Y, Du J, Rubtsov YP, Rudensky AY, Ziegler SF, Littman DR: TGF-beta-induced Foxp3 inhibits T(H)17 cell differentiation by antagonizing RORgammat function. Nature 2008, 453:236–240
54. Kim YH, Choi BK, Shin SM, Kim CH, Oh HS, Park SH, Lee DG, Lee MJ, Kim KH, Vinay DS, Kwon BS: 4-1BB triggering ameliorates experimental autoimmune encephalomyelitis by modulating the balance between Th17 and regulatory T Cells. J Immunol 2011, 187: 1120–1128
55. Beurel E, Yeh WI, Michalek SM, Harrington LE, Jope RS: Glycogen synthase kinase-3 is an early determinant in the differentiation of pathogenic Th17 cells. J Immunol 2011, 186:1391–1398
56. Guo X, Ramirez A, Waddell DS, Li Z, Liu X, Wang XF: Axin and GSK3- control Smad3 protein stability and modulate TGF- signaling. Genes Dev 2008, 22:106–120
57. Caraci F, Gili E, Calafiore M, Failla M, La Rosa C, Crimi N, Sortino MA, Nicoletti F, Copani A, Vancheri C: TGF-beta1 targets the GSK-3beta/beta-catenin pathway via ERK activation in the transition of human lung fibroblasts into myofibroblasts. Pharmacol Res 2008, 57:274–282
58. Wrighton KH, Lin X, Feng XH: Phospho-control of TGF-beta superfamily signaling. Cell Res 2009, 19:8–20
59. Martin M, Rehani K, Jope RS, Michalek SM: Toll-like receptor-mediated cytokine production is differentially regulated by glycogen synthase kinase 3. Nat Immunol 2005, 6:777–784
60. Bourguignon LY, Singleton PA, Zhu H, Zhou B: Hyaluronan promotes signaling interaction between CD44 and the transforming growth factor beta receptor I in metastatic breast tumor cells. J Biol Chem 2002, 277:39703–39712
61. Nijenhuis N, Mizuno D, Spaan JA, Schmidt CF: Viscoelastic response of a model endothelial glycocalyx. Phys Biol 2009, 6:025014
62. Kaya G, Rodriguez I, Jorcano JL, Vassalli P, Stamenkovic I: Selective suppression of CD44 in keratinocytes of mice bearing an antisense CD44 transgene driven by a tissue-specific promoter disrupts hyaluronate metabolism in the skin and impairs keratinocyte proliferation. Genes Dev 1997, 11:996–1007
63. Cinamon G, Grabovsky V, Winter E, Franitza S, Feigelson S, Shamri R, Dwir O, Alon R: Novel chemokine functions in lymphocyte migration through vascular endothelium under shear flow. J Leukoc Biol 2001, 69:860–866
64. Madri JA, Graesser D: Cell migration in the immune system: the evolving inter-related roles of adhesion molecules and proteinases. Dev Immunol 2000, 7:103–116
65. Takahashi K, Eto H, Tanabe KK: Involvement of CD44 in matrix metalloproteinase-2 regulation in human melanoma cells. Int J Cancer 1999, 80:387–395
66. Yu Q, Stamenkovic I: Cell surface-localized matrix metalloproteinase-9 proteolytically activates TGF-beta and promotes tumor invasion and angiogenesis. Genes Dev 2000, 14:163–176
67. Yang Y, Rosenberg GA: MMP-mediated disruption of claudin-5 in the blood-brain barrier of rat brain after cerebral ischemia. Methods Mol Biol 2011, 762:333–345
68. Esparza J, Kruse M, Lee J, Michaud M, Madri JA: MMP-2 null mice exhibit an early onset and severe experimental autoimmune encephalomyelitis due to an increase in MMP-9 expression and activity. FASEB J 2004, 18:1682–1691
69. Abbott NJ, Ronnback L, Hansson E: Astrocyte-endothelial interactions at the blood-brain barrier. Nat Rev Neurosci 2006, 7:41–53